Aalborg Universitet

AALBORG UNIVERSITY

Influence of nearby obstacles on the feasibility of a Huygens box as a field source

Franek, Ondrej; Sørensen, Morten; Ebert, Hans; Pedersen, Gert Frølund

[Link to publication from Aalborg University](#)

Citation for published version (APA):
Franek, O., Sørensen, M., Ebert, H., & Pedersen, G. F. (2012). Influence of nearby obstacles on the feasibility of a Huygens box as a field source. In *2012 IEEE International Symposium on Electromagnetic Compatibility Proceedings* (pp. 600-604). IEEE (Institute of Electrical and Electronics Engineers). https://doi.org/10.1109/ISEMC.2012.6351693

Influence of Nearby Obstacles on the Feasibility of a Huygens Box as a Field Source

Ondřej Franek [1], Morten Sørensen [2], Hans Ebert [3], Gert Frølund Pedersen [4]

Antennas, Propagation and Radio Networking, Department of Electronic Systems,
Faculty of Engineering and Science, Aalborg University
Niels Jernes Vej 12, 9220 Aalborg Øst, Denmark
[1] `of@es.aau.dk`
[2] `mos@es.aau.dk`
[3] `heb@es.aau.dk`
[4] `gfp@es.aau.dk`

Abstract—A method of substituting an electronic module with its Huygens box representation for the purpose of calculating the emitted field is discussed. It is pointed out that nearby obstacles may have harmful effect on the accuracy of such method. This is subsequently proven by performing finite-difference time-domain simulations on a simplified model of a printed circuit board (PCB) with a parallel open-ended cable in the vicinity. A solution to the problem is proposed: inclusion of the reduced model of the module inside the Huygens box, e.g. only the ground plane of the PCB. It is demonstrated that the described solution has the potential to decrease the errors to acceptable levels.

I. Introduction

Methods of replacing an electronic module with equivalent sources in order to calculate the surrounding electromagnetic fields have recently gained considerable attention in the EMC community [1], [2], [3]. The equivalent sources can serve as a substitute for the electronic module in numerical calculations. The goal is to be able to predict interference and radiation of the module, when it is mounted inside an apparatus before it is manufactured.

One approach to characterize the module is to scan the tangential near fields on a surface entirely enclosing the module. These fields distributed on the closed surface, the *Huygens box* (HB), then act as sources generating the same fields as the original module outside of this surface. Aside from difficulties connected with the measurement of the fields, this method has one theoretical limitation following from the definition itself: the fields are correctly reproduced only if there is free space everywhere around HB [4]. Clearly, this limitation goes against the very purpose of the undertaking, namely to be able to obtain fields with the apparatus and other obstacles around.

Since we planned to use this method for investigating intra-device EMI carried over cables running next to a module, we were interested in whether the HB method can provide trustable results. To this end, we decided to arrange a numerical experiment, supported by measurements in an anechoic chamber: a simplified test printed circuit board (PCB) generates fields in the presence of a parallel running open-ended cable. The objective is to find out how much will replacing

the PCB with Huygens sources change the surrounding fields, thus validating this approach for subsequent detailed analyses.

In Section II a brief overview of the theoretical background of the method is presented. Section III describes the numerical experiment and introduces the error metrics that were used in the evaluation. Results are shown and discussed in Section IV. Finally, conclusions are presented in Section V.

II. Theoretical background

The HB method is derived from Love's equivalence principle [4]. A structure containing sources and linear materials generates electromagnetic fields in free space. Tangential components of electric (E-) and magnetic (H-) fields are observed and recorded on a surface entirely enclosing the structure. Then, fields outside of this closed surface can be recreated by allowing equivalent electric and magnetic surface currents to run over the surface, whereas fields inside of the surface are zero and the radiating structure is removed. These currents are related to the original fields $\vec{E}$ and $\vec{H}$ on the surface by

$$\vec{J}_s = \hat{n} \times \vec{H}, \qquad \vec{M}_s = -\hat{n} \times \vec{E}, \qquad (1)$$

where $\hat{n}$ denotes normal vector oriented outwards the surface.

The tangential fields of a real-world structure, e.g. an electronic module, are usually obtained by measurement on conditions which are intended to be approaching free space, i.e. far from any obstacles. The fields are then converted to the surface currents by (1) and these will radiate the same fields as before. However, when an obstacle is introduced, a cable running next to the module for example, the situation changes. The cable may become coupled with the module and produce fields that are different from the original fields. The important point is that when HB is used to excite the cable, the module is not present inside the box and the cable has nothing to couple to, it "sees" only free space inside the box. The assumption is, therefore, that the fields recreated using HB will differ from the actual fields.

The aim of the numerical experiment presented below is to find out whether the fields will deviate dramatically, and if so, whether the problem can be mitigated in some way. One solution that is offering itself from the explanation above
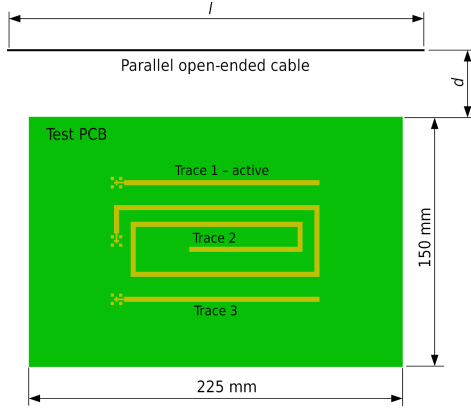
Fig. 1. Layout of the test PCB and position of the cable

is to return the module (without sources though) as a model back inside HB, or, if detailed information on the structure is unavailable, try to recreate its main features at least. This should provide the cable with a "companion" to couple to and bring the fields back near the original solution.

III. NUMERICAL EXPERIMENT

A. Test Setup

The simulated setup is shown in Fig. 1. The radiating structure in question is represented by a simplified test PCB with dimensions 225×150 mm, with three 3 mm wide traces on the top layer and a continuous metallic layer on the bottom. Only the first trace is excited, and the source and load impedances are identically 50 Ω, matching the characteristic impedance of the trace. The substrate is 2 mm thick and made of laminate of type FR4 (*flame resistant*), with relative permittivity set to 4.35 in the simulation.

The cable running next to the module is modeled by a straight metallic wire, placed along the edge of the test PCB parallel to the active trace and opened at both ends. Distance of the cable from the PCB d has been varied in 20 mm steps up to 100 mm, and its length l has been spanning the interval 50–300 mm by 50 mm steps.

B. Simulations

The simulation has been carried out with an in-house numerical code implementing the finite-difference time-domain (FDTD) method [5], with resolution of 1 mm and perfectly matched layers as the absorbing boundary condition. Losses in metals and the substrate have been neglected in the simulation. Near fields (up to 30 mm from both structures) and far fields (extrapolated to infinity) have been calculated for 100 MHz, 500 MHz and 1 GHz.

There are three distinct scenarios to be observed (see Fig. 2):

a) The test PCB without obstacle: (Fig. 2a) No obstacle is present and the fields generated by the PCB are recorded to serve as a basis for HB, similarly to near field scanning measurement.
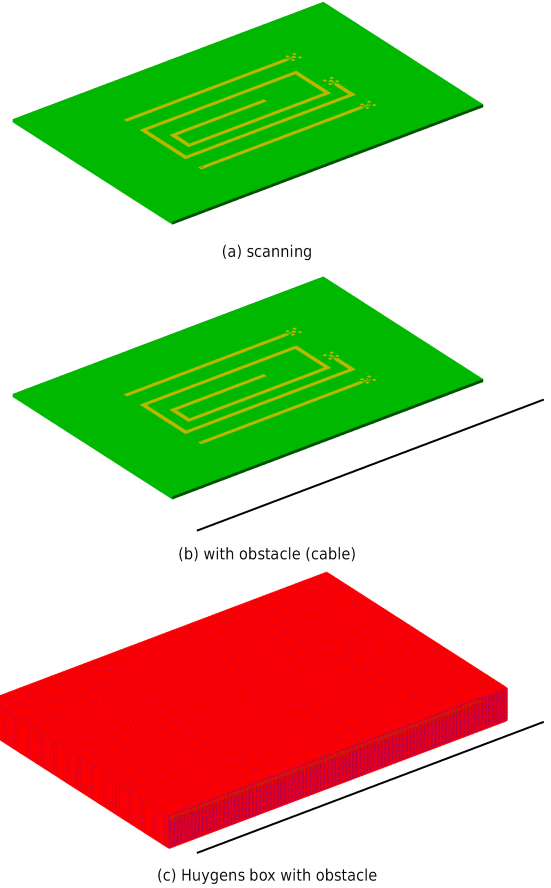

(a) scanning

(b) with obstacle (cable)

(c) Huygens box with obstacle

Fig. 2. Simulation scenarios

b) The test PCB with the cable: (Fig. 2b) This is the reference case, as the fields produced in this case are the ones we desire to know.

c) HB with the cable: (Fig. 2c) Here the PCB is replaced by the equivalent sources flowing on the surface of HB, which were obtained via (1) from scenario *a*. The sources are positioned at a fixed distance of 10 mm from the original PCB in all directions, hence the box has dimensions $245 \times 170 \times 22$ mm. The inside of HB can be empty, or it can contain full or reduced complexity model of the PCB *sans* sources (see Section IV). This scenario will be compared to scenario *b*.

C. Error Metrics

To be able to compare the results with enough robustness, we introduce following expressions for errors: the total error in near field (for both E- and H-fields), the total error in far field (E-field only), the amplitude error in far field (E-field only), and the equivalent signal-to-noise ratio (SNR) as a complement to each of the previous errors.

1) Total error in near field: The total error in near field is defined as the peak modulus of the difference between scenarios *b* and *c*, divided by peak modulus of the correct

field b

$$\text{Total error} = 100 \times \frac{\max |F^{(c)} - F^{(b)}|}{\max |F^{(b)}|} \; [\%], \qquad (2)$$

where F stands for the vector magnitude of E or H field everywhere in the computational domain outside HB. The division by the peak value ensures that the error is not unreasonably high in areas where the intensities are negligible. In addition, the formulation detects also changes in phase of the fields which may be important for coupling and radiation.

2) Total error in far field: In the far field, the two perpendicular field components (polarizations) are treated separately. Peak values of fields and their errors are found for each component, θ and ϕ, of the E-field, and the higher value of the two is chosen for the metric

$$\text{Total error} = 100 \times$$
$$\frac{\max \left(\max |E_\theta^{(c)} - E_\theta^{(b)}|, \max |E_\phi^{(c)} - E_\phi^{(b)}| \right)}{\max \left(\max |E_\theta^{(b)}|, \max |E_\phi^{(b)}| \right)} \; [\%]. \quad (3)$$

The denominator selects also the higher of the two polarizations—this way we can eliminate large errors (from division by small numbers) in cases when one of the field polarizations is very small. The phase of the error is again detected.

3) Amplitude error in far field: This is a variation of the previous metric, where we do not take the phase into account and subtract the moduli only (note the addition of extra $| \ldots |$ operators)

$$\text{Amplitude error} = 100 \times$$
$$\frac{\max \left(\max ||E_\theta^{(c)}| - |E_\theta^{(b)}||, \max ||E_\phi^{(c)}| - |E_\phi^{(b)}|| \right)}{\max \left(\max |E_\theta^{(b)}|, \max |E_\phi^{(b)}| \right)} \; [\%]. \quad (4)$$

The formulation of the amplitude error (4) has been designed to indicate changes in radiated emission as detected by standardized measurement techniques where the phase is not important.

4) Signal-to-noise ratio: Introduction of error by replacing the original PCB with HB can be likened to adding a noise in the observed fields. Whereas the original fields have infinite SNR (because they are assumed to be exact), the fields generated by HB will have certain noise caused by the errors. For any percentage error presented above, the SNR figure of merit can be expressed as

$$\text{SNR} = -20 \log_{10} \frac{\text{error}}{100} \; [\text{dB}]. \qquad (5)$$

Using this metric we can see the fields generated by HB as having the correct value, but with certain noise due to the imperfection of the source model superimposed on top of it and related to the peak value of the fields by the SNR number.

IV. Results and Discussion

We simulated and compared scenarios b and c for various distances and lengths of the cable. Figs. 3 and 4 show the total errors given by (2) in E and H components of the near field, respectively, at 1 GHz when HB is empty. Both plots have similar tendencies: the errors tend to be higher when the cable is closer to the PCB (strong coupling) and peak at lengths of the cable which correspond to resonances for the given frequency. The difference in error values between E and H fields, 47 % versus 29 %, can possibly be attributed to different total levels in each component—if the magnetic fields are stronger in this case, the error will appear smaller in percentage.
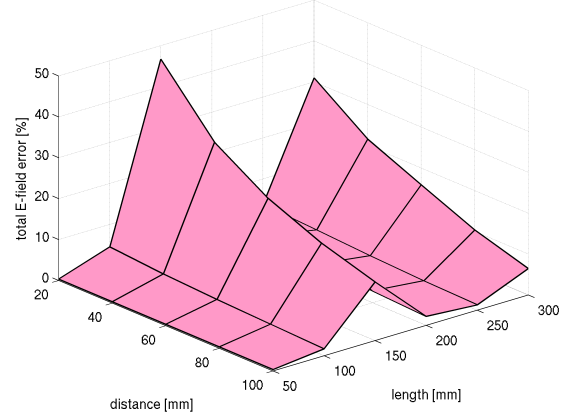

Fig. 3. Total E-field error at 1 GHz when HB is empty
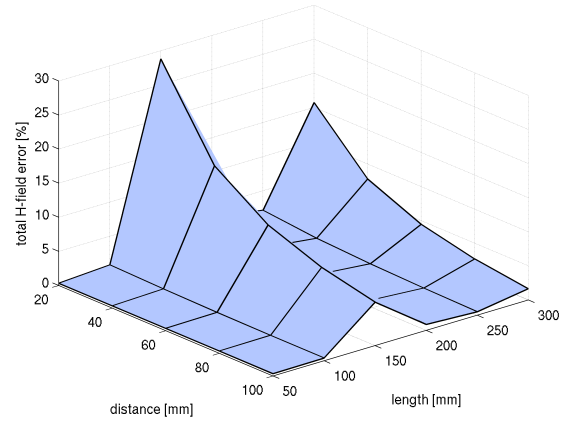

Fig. 4. Total H-field error at 1 GHz when HB is empty

Since the errors are quite significant when the Hyugens box is empty, we tried to include the metallic ground plane of the test PCB as the expectedly most influential feature inside HB, hoping to reduce the errors. And indeed, by reintroducing the ground plane inside HB the errors dropped below 5 %, as shown in Figs. 5 and 6.

For final comparison, only maximum errors across all dimensions of the cable have been selected. The near-field errors and SNR, together with the dimensions at which the maximum error occurred, are displayed in Table I. Again, it

Frequency	HB Scenario	E-field			H-field		
		Total Error [%]	SNR [dB]	Cable Dimensions [mm]	Total Error [%]	SNR [dB]	Cable Dimensions [mm]
100 MHz	Empty	0.40	48	d = 20, l = 200	0.072	63	d = 20, l = 300
	With ground plane inside	0.030	70	d = 20, l = 300	0.030	70	d = 20, l = 300
	With full PCB model inside	0.029	71	d = 20, l = 150	0.027	71	d = 20, l = 50
500 MHz	Empty	71	3.0	d = 20, l = 300	72	2.8	d = 20, l = 300
	With ground plane inside	13	18	d = 20, l = 300	13	18	d = 20, l = 300
	With full PCB model inside	0.14	57	d = 20, l = 300	0.14	57	d = 20, l = 300
1 GHz	Empty	47	6.6	d = 20, l = 150	29	11	d = 20, l = 150
	With ground plane inside	4.2	28	d = 20, l = 300	2.0	34	d = 20, l = 300
	With full PCB model inside	1.9	34	d = 60, l = 300	0.91	41	d = 20, l = 150

| Frequency	HB Scenario	Total Error [%]	SNR [dB]	Cable Dimensions [mm]	Amplitude Error [%]	SNR [dB]	Cable Dimensions [mm]
100 MHz	Empty	0.33	50	d = 20, l = 300	0.33	50	d = 20, l = 300
	With ground plane inside	0.015	76	d = 20, l = 300	0.011	79	d = 20, l = 300
	With full PCB model inside	0.0058	85	d = 20, l = 150	0.0022	93	d = 40, l = 300
500 MHz	Empty	77	2.3	d = 20, l = 300	56	5.0	d = 40, l = 300
	With ground plane inside	16	16	d = 20, l = 300	9.9	20	d = 20, l = 300
	With full PCB model inside	0.21	53	d = 20, l = 300	0.15	56	d = 20, l = 300
1 GHz	Empty	11	19	d = 20, l = 150	11	19	d = 40, l = 150
	With ground plane inside	0.92	41	d = 20, l = 300	0.90	41	d = 20, l = 300
	With full PCB model inside	1.4	37	d = 20, l = 150	0.32	50	d = 20, l = 150
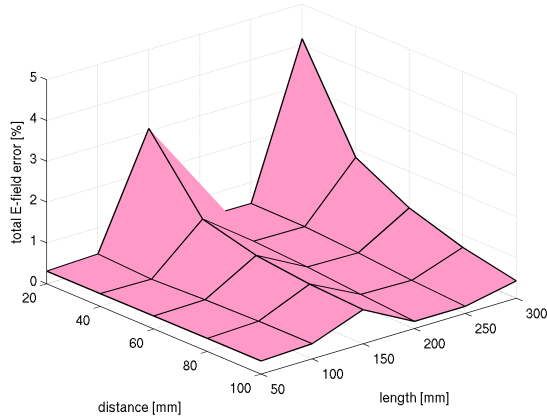
Fig. 5. Total E-field error at 1GHz when the ground plane of the PCB is present inside HB
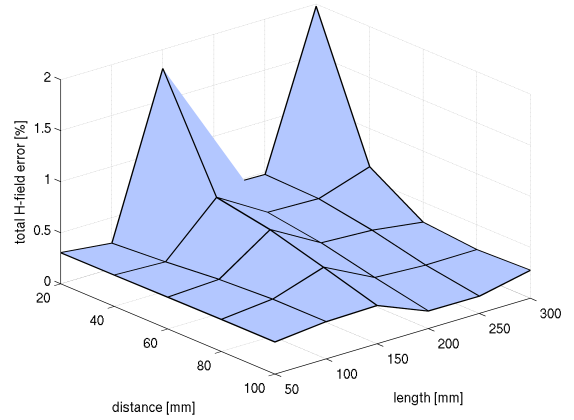

Fig. 6. Total H-field error at 1GHz when the ground plane of the PCB is present inside HB

can be clearly seen that including the model of the PCB inside HB has a strong beneficial effect on the quality of the fields.

If the model is absolutely accurate (denoted as "full PCB model" in Tables I and II), the errors drop to negligible levels. In our simulations of this case we utilized the same PCB model as in scenario *a* (Fig. 2a), but we removed the feed source and placed the model inside HB. Thus, the medium is kept identical everywhere in the domain (including the cable), only the feed source is replaced by the sources running over the surface of HB.

But even if the model inside the HB is very crude, such as if the PCB is represented by its ground plane only, the error is still acceptable for wide range of problems. In fact, the observed numbers suggest a tendency according to which the error should converge to negligible levels when the sourceless model inside HB converges to the original radiating structure. There will be a tradeoff between the error and the complexity of the PCB model whose exact parameters (dimensions, materials, etc.) may be cumbersome or otherwise difficult to obtain.

Further observation tells us that the highest errors occur when the cable is closest to the PCB and has resonant length at the particular frequency. This rule does not apply only when the error is very small, because then it probably has a flat, random-like profile across the dimensions.

Table II shows the total and amplitude errors in the far fields. Similar conclusions can be drawn as for the near fields. It is worth noting that an amplitude error of 50 % means at most 6 dB drop or 3.5 dB increase in the peak radiation with respect to the exact scenario. From this point of view, the HB method may in many situations be suitable for radiation prediction *as is*, without including any model inside the box, since it would be under- or overestimating the true radiated levels by still acceptable margin.

V. Conclusion

In this paper, we have compared scenario of a PCB model and a nearby cable with similar scenario where the PCB is replaced by HB. We have seen that such replacement, although bringing advantages into interference tracking, can carry a burden of significant errors in emitted fields. However, errors can be dramatically reduced if main features of the PCB are reinserted into HB, as has been demonstrated with the example of the PCB ground plane. If the model of the structure is converging to the full original model, excluding the sources, then, correspondingly, the error can be made almost negligible.

It can therefore be concluded that HB may be used as a field source in simulations, but only if the inside of HB is also taken into account. If the findings obtained for the PCB and the cable can be generalized to any combination of structures, this may eventually open the door for successful application of the HB method for accurately predicting inter- and intra-device interference in complex environments.

References

[1] Y. Vives-Gilabert, C. Arcambal, A. Louis, F. de Daran, P. Eudeline, and B. Mazari, "Modeling magnetic radiations of electronic circuits using near-field scanning method," *IEEE Trans. Electromagn. Compat.*, vol. 49, no. 2, pp. 391–400, May 2007.

[2] X. Tong, D. W. P. Thomas, A. Nothofer, P. Sewell, and C. Christopoulos, "Modeling electromagnetic emissions from printed circuit boards in closed environments using equivalent dipoles," *IEEE Trans. Electromagn. Compat.*, vol. 52, no. 2, pp. 462–470, May 2010.

[3] H. Weng, D. G. Beetner, and R. E. DuBroff, "Prediction of radiated emissions using near-field measurements," *IEEE Trans. Electromagn. Compat.*, vol. 53, no. 4, pp. 891–899, Nov. 2011.

[4] C. A. Balanis, *Advanced Engineering Electromagnetics*. New York: Wiley, 1989.

[5] A. Taflove and S. C. Hagness, *Computational Electrodynamics: The Finite-Difference Time-Domain Method*, 3rd ed. Boston: Artech House, 2005.